

## RESEARCH ARTICLE

# Enhancing Solid Oxide Fuel Cell Efficiency Through Advanced Model Identification Using Differential Evolutionary Mutation Fennec Fox Algorithm

Manish Kumar Singla<sup>2,3</sup> · Jyoti Gupta<sup>4</sup> · Ramesh Kumar<sup>1,5</sup> · Pradeep Jangir<sup>6,7,8</sup> · Mohamed Louzazni<sup>9</sup> · Nimay Chandra Giri<sup>10</sup> · Ahmed Jamal Abdullah Al-Gburi<sup>11,14</sup> · E. I.-Sayed M. El-Kenawy<sup>12</sup> · Amal H. Alharbi<sup>13</sup>

Received: 16 October 2024 / Accepted: 5 February 2025

© The Author(s) 2025

## Abstract

Fuel cells (FCs) are increasingly attracting attention for their efficient conversion of chemical energy into electricity without the need for combustion. Their high efficiency and versatility make them a promising technology across various applications. Researchers are actively exploring ways to optimize FC systems to meet specific energy needs. Among the different types of fuel cells, solid oxide fuel cells (SOFCs) stand out as a promising clean energy technology that generates electricity through electrochemical reactions. However, accurately modeling SOFCs, which is essential for reducing design costs, presents a challenge due to their complex and nonlinear characteristics. An ideal model should be adaptable to varying operating pressures and temperatures. This research introduces a novel approach for optimal SOFC model identification using a differential evolutionary mutation Fennec fox algorithm (DEMFFA). A real-world case study demonstrates the superior effectiveness of DEMFFA compared to existing methods. Additionally, a sensitivity analysis evaluates the influence of temperature and pressure on the model, with results indicating that the proposed method achieves higher efficiency than other approaches. The sum of the square error of the proposed algorithm is  $1.18\text{E}-11$  followed by the parent algorithm, Fennec fox algorithm (FFA) ( $1.24\text{E}-09$ ), and some of the compared algorithms. The computational time of the proposed algorithm is 1.001 s, followed by the parent algorithm FFA (1.199 s) and some of the compared algorithms. DEMFFA offers significant potential, enhancing renewable energy, minimizing SOFC's environmental impact, and improving real-world applications like distributed power generation and hydrogen integration.

**Keywords** Mathematical modeling · Optimization · Fuel cells · Statistical tests · Renewable energy

## 1 Introduction

The escalating need for cleaner power generation is driving the demand for innovative energy technologies [1, 2]. Fuel cells, renowned for their efficient and responsive performance, are emerging as a promising solution. Their advantages in terms of location flexibility, power quality, reliability, and portability are accelerating their adoption [3]. Operating on electrochemical principles, fuel cells produce direct current electricity. Common types include phosphoric acid, polymer membrane, alkaline, molten carbonate, and solid oxide fuel cells (SOFCs) [4,



5]. Key factors propelling fuel cell commercialization are fuel availability, operational flexibility, and tolerance to pollutants [6].

Hydrogen fuel cells operate by accumulating hydrogen at the anode and oxygen at the cathode. A catalyst splits hydrogen molecules into protons and electrons [7]. While protons migrate through the electrolyte, electrons are prevented from doing so, forcing them to travel through an external circuit, generating electricity. This process produces heat and water as by-products and continues as long as hydrogen is available. At the fuel cell's anode, hydrogen undergoes oxidation, releasing electrons that flow through an external circuit to the cathode [8, 9]. The positively charged hydrogen ions (protons) migrate through the electrolyte membrane to the cathode. Here, they combine with oxygen and electrons from the external circuit and catalyzed to produce water [10].

Fuel cell technology is a promising clean energy solution capable of converting chemical energy directly into electricity and heat. Renowned for its efficiency, quiet operation, versatility, and low emissions, fuel cell technology is a multidisciplinary field with vast potential across various sectors [11]. Its impact extends to transportation, energy, and the environment. Fuel cells can be categorized into several types based on their electrolyte and operating conditions, including solid oxide fuel cells (SOFCs), which are particularly noteworthy for their ability to generate electricity efficiently. Solid oxide fuel cells (SOFCs) offer high efficiency in converting natural gas into electricity [12–14]. Under optimal conditions, they can achieve energy conversion rates of nearly 90%. However, modeling these systems is a complex challenge due to the simultaneous occurrence of mass transport, electrical charge movement, heat transfer, and electrochemical reactions within each cell [15–20].

Several factors, including temperature, electrolyte composition, thickness, and electrode porosity, significantly impact SOFC performance, compounding the complexity of modeling [21]. Accurately determining fuel cell parameters is a primary challenge, as modifying one parameter often influences multiple others, sometimes adversely. Despite these hurdles, extensive research has been dedicated to addressing these complexities [13, 22].

El-Hay et al. [23] used the satin bowerbird optimization technique to study SOFC steady-state and dynamic approaches. This work presents an efficient method based on a specialized version of the satin bowerbird optimizer (SBO) algorithm for accurately characterizing SOFCs. The test function is modified to minimize the mean squared deviations (MSD) between the computed and monitored output voltages of stacked SOFCs. The SBO's excellent performance is demonstrated by the negligible MSD values in the three test instances investigated. The solid oxide fuel cells (SOFCs) has shown the efficacy of this technique by achieving high marks for developing competitive qualities for both dynamic and steady-state methods. However, it is important to note that there is always room for improvement in the SOFC approach.

To extract SOFC parameters, Yang et al. [24] proposed an extreme learning machine that utilizes meta-heuristic approaches. This ground breaking method aims to extract unknown variables from electrochemical and fundamental electrochemical SOFC techniques. Simulation results showed that the proposed method significantly aids in determining the model's optimal parameters while offering high accuracy, notable reliability, maximum speed, and exceptional durability. Specifically, the variable extraction accuracy of the electrochemical modeling and basic electrochemical approach may be improved by up to 65.6% and 49.3%, respectively.

Recent scientific efforts have centered on enhancing the accuracy of parameter estimation for solid oxide fuel cells (SOFCs). Alhumade et al. [25] utilized sophisticated optimization techniques to determine the optimal values for key SOFC parameters. Azar et al. [26] introduced a groundbreaking battle royale optimization model designed to identify uncertain variables within the SOFC system. This innovative approach aimed to minimize the discrepancies between simulated and real-world voltage data. The model's effectiveness was validated through successful application to a 96-cell SOFC stack under diverse operating conditions, outperforming traditional methods.

Bai et al. [27] proposed a novel approach to optimize the operating parameters of solid oxide fuel cells (SOFCs) by combining cuckoo search and gray wolf optimization (CSGWO) algorithms. This hybrid optimization technique efficiently pinpointed critical SOFC variables through rapid convergence. By minimizing the mean squared deviation (MSD) between predicted and actual values, CSGWO demonstrated superior performance compared to other optimization methods. The model's exceptional predictive accuracy was confirmed by the lowest mean squared error (MSE) values observed for operating pressures across various scenarios. These results highlight

the potential of cuckoo search and gray wolf optimization (CSGWO) as a promising tool for accurate parameter estimation in SOFC systems.

Existing optimization techniques, such as sine-based optimization (SBO), chaotic salp swarm algorithm (CSSA), particle swarm optimization (PSO), and honey badger algorithm (HBA), often face limitations in complex parameter estimation tasks. SBO and CSGWO can suffer from premature convergence or an imbalance between exploration and exploitation. PSO often exhibits slow convergence and may get stuck in suboptimal solutions. While HBA can be effective, it may have limited adaptability. These limitations necessitate the development of more robust algorithms. The proposed differential evolutionary modified Fennec fox algorithm (DEMFFA) addresses these challenges by incorporating enhanced mechanisms like sine chaotic mapping, cosine adjustment, and Cauchy mutation. These mechanisms improve search space exploration and exploitation, ensuring higher accuracy and reliability in complex optimization scenarios.

Hydrogen, with its clean energy profile and high conversion efficiency, is a cornerstone for a sustainable energy future. Solid oxide fuel cells (SOFCs), capable of efficiently transforming chemical energy into electricity, have emerged as a promising technology for hydrogen utilization. However, the intricate nature and complex interactions within SOFC systems pose significant challenges in developing accurate and reliable models [28, 29]. The high operating temperatures (typically 600–1000 °C) necessitate specialized and expensive materials for construction and maintenance. This elevated temperature environment accelerates material degradation, leading to reduced performance and shortened lifespan. Components such as interconnects and seals are particularly susceptible to thermal stresses and chemical reactions, requiring frequent inspections and potential replacements. The scaling up of SOFC systems for industrial applications presents considerable engineering challenges. Ensuring consistent performance and reliability across large-scale arrays is crucial, while maintaining cost-effectiveness remains a major obstacle. These practical challenges underscore the critical importance of accurate and efficient modeling. By simulating the behavior of SOFC systems under various operating conditions and predicting potential degradation mechanisms, researchers and engineers can optimize designs, minimize maintenance requirements, and accelerate the path towards commercialization.

To advance SOFC technology, sophisticated modeling techniques and adaptive parameter identification methods are essential for accurate performance prediction. Current limitations include a lack of precise models capturing cell stack behavior, particularly electrical coupling effects, and deficiencies in existing parameter identification approaches. Traditional optimization techniques often struggle in complex scenarios, particularly those with high-dimensional parameter spaces. These methods frequently encounter challenges such as slow convergence, premature convergence, and difficulties in adapting to changing conditions. This gap in performance highlights the need for more robust and efficient algorithms such as DEMFFA, which can effectively navigate complex search spaces and deliver reliable solutions across a range of operating conditions. This research addresses these challenges by providing a comprehensive overview of SOFC modeling and parameter identification technologies, offering insights for future advancements. The paper's key contribution is outlined in the following highlights.

- The parameters of the SOFC model are optimally extracted using a unique DEMFFA approach.
- Real-world experiments validate new technique's performance across environments against established methods.
- Temperature and pressure variations is also found out to assess the proposed algorithm's consistency and robustness.

## 1.1 Motivation

Our innovative research has significantly advanced the field of SOFC modeling by introducing a revolutionary new approach, DEMFFA. Through meticulous optimization of key parameters, we have achieved unparalleled levels of accuracy and reliability in our simulations. Rigorous real-world testing has unequivocally demonstrated

the superiority of our technique compared to existing methods. Our algorithm has proven to be highly robust and consistent, performing exceptionally well across a wide range of environmental conditions, from extreme heat to freezing cold. This breakthrough represents a significant leap forward in the pursuit of sustainable energy solutions.

## 2 SOFC Modeling

Fuel cells are like power plants that create electricity through a continuous chemical reaction. Instead of burning fuel like a traditional engine, they use a process similar to a battery, but without storing energy themselves. They constantly need a supply of fuel and oxygen to keep producing electricity. Unlike engines, fuel cells are clean and efficient because they do not release harmful greenhouse gases [30]. Solid oxide fuel cells (SOFCs) are a type of high-temperature fuel cell that operates around 1000°C [31] and uses hydrogen as fuel and oxygen from the air. An SOFC has three main parts:

The chemical reaction of anode side is:



The chemical reaction of cathode side is:

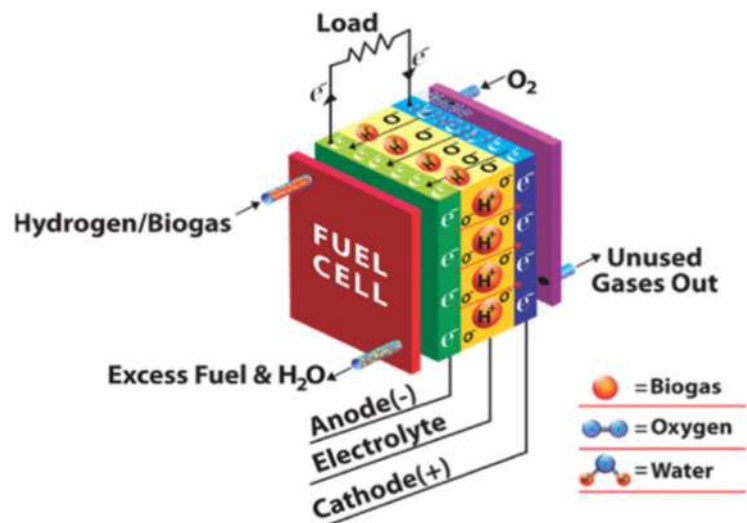


The electrochemical overall reaction is:



At the cathode of a solid oxide fuel cell (SOFC), oxygen molecules undergo reduction to form negative oxygen ions. These special ions can travel through the electrolyte, but electrons cannot. On the fuel side (anode), hydrogen reacts with these incoming negative ions, creating water vapor and releasing electrons. These electrons then flow through the external circuit connected between the anode and cathode, powering your devices. Figure 1. [32] shows a diagram of an SOFC.

**Fig. 1** SOFC schematic



A single SOFC cell's output voltage ( $V_{cell}$ ) can be calculated using Eq. 4 [33]. This equation considers two factors: the theoretical maximum voltage based on the fuel cell's chemistry (called the Nernst potential), and the voltage lost due to various inefficiencies within the cell during the energy conversion process.

$$V_{Cell} = E_{nernst} - (\text{all losses in a fuel cell}). \quad (4)$$

The ideal voltage a hydrogen/oxygen fuel cell can produce under real-world conditions is calculated using the Nernst equation (shown in Eq. 5). This equation takes into account several factors that affect the cell's performance [40]:

$$E_{nernst} = E_o + \frac{RT}{2F} \ln \left( \frac{P_{H_2} \times \sqrt{P_{O_2}}}{P_{H_2O}} \right). \quad (5)$$

Reversible standard potential ( $E_o$ ): this represents the theoretical maximum voltage of a cell under specific standard conditions. Universal gas constant ( $R$ ): this constant relates temperature, pressure, and the amount of gas (often denoted by 8.3145 J/mol/K). Faraday constant ( $F$ ): this constant relates the amount of electrical charge to the amount of chemical reaction (often denoted by 96,485 C/mol).

Solid oxide fuel cells (SOFCs) experience three main types of voltage losses that affect their overall efficiency. Activation loss: This loss happens at the start of the reaction because energy is needed to overcome a hurdle before the fuel and oxygen can interact. This loss is influenced by operating conditions and can be calculated using the Butler–Volmer equation (shown in Eq. 6). Ohmic loss: This loss is similar to resistance in a wire. It occurs because the materials in the SOFC have some resistance to the flow of ions, leading to a voltage drop. This loss depends on the operating temperature and materials used in the cell. Concentration overpotential loss: This loss happens when the fuel or oxygen supply cannot keep up with the demand at the electrodes. This can be caused by high current draw or limitations in gas flow.

$$V_{activation} = A \sinh^{-1} \left( \frac{J_{load}}{2J_{o,a}} \right) + A \sinh^{-1} \left( \frac{J_{load}}{2J_{o,c}} \right). \quad (6)$$

$J_{load}$ ,  $J_{o,a}$ , and  $J_{o,c}$  are the load current density, anode exchange current density, and cathode exchange current density, in mA/cm<sup>2</sup>, respectively. The slope of the Tafel line is represented by the symbol  $A$ .

Ohmic loss is a voltage drop caused by resistance to the flow of electricity within the SOFC. This resistance comes from two sources: the difficulty for charged particles (ions) to move through the electrolyte; the resistance of the cell's electrodes to electron flow. Equation 7 can be used to calculate this ohmic loss.

$$V_{ohmic} = J_{load} R_{ohm}, \quad (7)$$

where the ionic resistance is denoted by  $R_{ohm}$ .

During the process, concentration gradients cause  $V_{concentration}$ , or concentration loss. When the operational current density approaches the current limit ( $J_{max}$ ), it is shown in Eq. 8 that:

$$V_{concentration} = -b \times \ln \left( \frac{J_{max} - J_{load}}{J_{max}} \right), \quad (8)$$

where  $b$  is an unknown parametric coefficient that varies depending on the operating parameters of the fuel cell.

Equations 9 and 10 determine the output voltage of an SOFC and give the resultant stack voltage of  $n_{\text{cell}}$  linked in series. As activation voltage loss, ohmic resistance and concentration loss are the primary losses that occur in fuel cell, whereas the rest of the losses are secondary losses which can be neglected, as these have quite low values and do not have much effect on the performance of the SOFC.

$$V_{\text{cell}} = E_{\text{nernst}} - (V_{\text{activation}} + V_{\text{ohmic}} + V_{\text{concentration}}), \quad (9)$$

$$V_{\text{stack}} = n_{\text{cell}} \times V_{\text{cell}}. \quad (10)$$

## 2.1 Formulating the Issue

This paper proposes a new algorithm to determine the optimal parameters for a solid oxide fuel cell (SOFC) model. The algorithm predicts the cell's output voltage at various current densities using optimization techniques. To assess the accuracy of these predictions, the sum of squared error (SSE) is used as the evaluation metric. Equation 11 details the objective function used for optimization.

$$\text{SSE} = \text{MIN} \left( F = \sum_{i=1}^N (V_{\text{actual}} - V_i)^2 \right). \quad (11)$$

In this study, the objective is to minimize the sum of square error (SSE) between the predicted output voltage ( $V_i$ ) using various optimization techniques and the experimental output voltage ( $V_{\text{actual}}$ ) to enhance the accuracy and precision of SOFC parameter estimation. The SSE is calculated using Eq. 11, where  $N$  represents the number of data points.

## 3 Fennec Fox Algorithm

The Fennec fox algorithm (FFA) is a nature-inspired meta-heuristic algorithm introduced by Eva Trojovsa et al. in 2022 [34]. It draws its inspiration from the Fennec fox's remarkable digging skills and its instinctive behavior of escaping from predators in the wild. These traits serve as the foundational concepts behind the development of the Fennec fox algorithm. Figure 2. provides an image of the Fennec fox.

### 3.1 Initialization

At the beginning of the process, fennec foxes are randomly placed in the search space using the random initialization formula (12).



**Fig. 2** Fennec foxes in nature [35]



$$Y_i : y_{ij} = lb_j + r \cdot (ub_j - lb_j), i = 1, 2, \dots, N, j = 1, 2, \dots, m. \quad (12)$$

Here,  $Y_i$  is the  $i$ th Fennec fox,  $N$  is the total number of Fennec foxes,  $m$  is the number of decision variables,  $r$  is a random number in the range  $[0, 1]$ , and  $lb$  and  $ub$  are the lower and upper bounds.

In Eq. (13),  $Y$  denotes the population matrix, encompassing the whole population of Fennec foxes.

$$Y = \begin{bmatrix} Y_1 \\ \vdots \\ Y_i \\ \vdots \\ Y_N \end{bmatrix}_{N \times M} = \begin{bmatrix} y_{1,1} & \cdots & y_{1,j} & \cdots & y_{1,m} \\ \vdots & \ddots & \vdots & \ddots & \vdots \\ y_{i,1} & \cdots & y_{i,j} & \cdots & y_{i,m} \\ \vdots & \cdots & \vdots & \ddots & \vdots \\ y_{N,1} & \cdots & y_{N,j} & \cdots & y_{N,m} \end{bmatrix}_{N \times m}, \quad (13)$$

where  $Y_i = (y_{i,1}, y_{i,2}, \dots, y_{i,m})$  represents the  $i$ th Fennec fox, with the column vector indicating the candidate value of the  $j$ th decision variable.

To solve for the objective function values of each Fennec fox, the vector method described in Eq. (14) was employed for modeling.

$$f = \begin{bmatrix} F_1 \\ \vdots \\ F_i \\ \vdots \\ F_N \end{bmatrix}_{N \times 1} = \begin{bmatrix} F(Y_1) \\ \vdots \\ F(Y_i) \\ \vdots \\ F(Y_N) \end{bmatrix}_{N \times 1}. \quad (14)$$

Here,  $f$  represents the vector that contains the values of the objective function, whereas  $F_i$  represents the value of the objective function for the  $i$ th Fennec fox.

### 3.2 Location Update

The position update stage for the Fennec foxes primarily revolves around their behavior of digging for prey and escaping from predators.

Phase 1: Exploitation: Prey Capture

During the prey hunting stage, the Fennec fox explores a field with a radius of  $r$ . This property enables the algorithm to approach the global optimal solution more closely. In the development stage, the mathematical model corresponding to the Fennec fox position update is as follows (Eqs. 15–17):

$$y_{ij}^{q1} = y_{ij} + (2 \cdot r - 1) \cdot r_{ij}, \quad (15)$$

$$r_{ij} = \alpha \cdot \left(1 - \frac{t}{l}\right) \cdot y_{ij}, \quad (16)$$

$$Y_i = \begin{cases} Y_i^{q1}, & F_i^{q1} < F_i \\ Y_i, & \text{else} \end{cases} \quad (17)$$

where  $Y_i^{q1}$  represents the new position of the  $i$ th Fennec fox in the first stage along the  $j$ th dimension,  $F_i^{q1}$  is the corresponding objective function value,  $t$  denotes the current number of iterations,  $l$  is the maximum number of iterations, and  $\alpha$  is a fixed constant with a value of 0.2.

### Phase 2: Exploration: Escaping Predators

During the predator evasion stage, the Fennec foxes' remarkable ability to escape helps the algorithm avoid being trapped in the local optima. In the exploration phase, the mathematical model for updating the Fennec foxes' positions is described by Eqs. (18–20).

$$Y_i^{rand} : y_i^{rand} = y_{kj}, k \in \{1, 2, \dots, N\}, i = 1, 2, \dots, N, \quad (18)$$

$$y_{i,j}^{q2} = \begin{cases} y_{i,j} + r \cdot (y_{i,j}^{rand} - I \cdot y_{i,j}), & F_i^{rand} < F_i \\ y_{i,j} + r \cdot (y_{i,j} - y_{i,j}^{rand}), & \text{else} \end{cases} \quad (19)$$

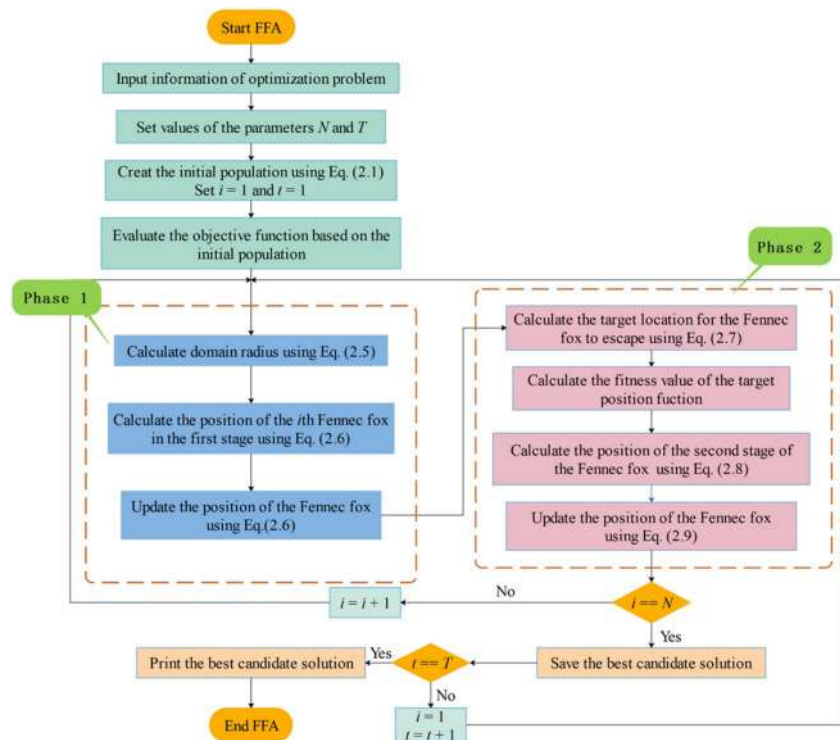
$$Y_i = \begin{cases} Y_i^{q2}, & F_i^{q2} < F_i \\ Y_i, & \text{else} \end{cases}, \quad (20)$$

where  $Y_i^{rand}$  represents the position to which the Fennec fox has escaped,  $F_i^{rand}$  is the corresponding objective function value,  $Y_i^{q2}$  denotes the updated position of the Fennec fox in the second stage,  $F_i^{q2}$  is the value of its objective function, and  $I$  is a random number selected from the set [1, 2].

Once the algorithm is fully initialized, it proceeds through Phase 1 and Phase 2, completing one iteration. Algorithm 1 provides the pseudo-code for the FFA, with steps 6–8 corresponding to the first stage of the algorithm, and steps 9–12 corresponding to the second stage. Figure 3 illustrates the flow diagram of the FFA.

Algorithm-1 [36]

**Fig. 3** FFA flowchart [35]





Begin FFA				
		Step 1: Initialization: Enter the relevant initialization parameters;		
		Step 2: Fitness calculation: The fitness value corresponding to each Fennec fox was calculated, and the current minimum moderate value $f$ was selected as the optimal value $f_{best}$ and the corresponding Fennec fox was recorded		
		Step 3: While t is less than the maximum number of iterations		
			for $i = 1 : N$	
				$R_{i,j} = \alpha \cdot (1 - \frac{iter}{Maxiter}) \cdot y_{i,j}$
				$Y_{new} = y_{i,j} + (2 \cdot r - 1) \cdot R(i, :)$
				if $f(Y_{new}) < f(Y_{best})$
				$Y_{best} = Y_{new}; f_{best} = f(Y_{new})$
				end if
			end for	
			$Y_{rand} = rand(Pop, Dim) \cdot y$	
			$I = I + rand$	
			for $i = 1$ to pop do	
				Calculate the fitness value of $Y_{rand}$
				if $f(Y_{rand}) < f(Y_{best})$
				$Y_{new} = y_{i,j} + rand \cdot (y_{rand} - I \cdot y_{i,j})$
				else
				$Y_{new} = y_{i,j} + rand \cdot (y_{i,j} - y_{rand})$
				else if
				if $f(Y_{new}) < f(Y_{best})$
				$Y_{best} = Y_{new}; f_{best} = f(Y_{new})$
				end if
			end for	
		end While		
	Step 4: Return: The optimal position $Y_{best}$ and fitness value $f(Y_{best})$ for Fennec Fox			
End FFA				

### 3.3 Fennec Fox Algorithm Improved Version

While the FFA demonstrates significant strengths in solving optimization problems, it does encounter certain challenges, such as the risk of getting stuck in local optima and limited performance in specific scenarios. To address these issues and further enhance the algorithm, a multi-strategy improved version of FFA, known as DEMFFA, is proposed. DEMFFA incorporates several strategies to overcome these limitations. DEMFFA seeks to address the shortcomings of the original FFA, enhancing its performance in terms of convergence speed and solution quality, and thereby strengthening its effectiveness in solving optimization problems.

#### 3.3.1 Sine Chaotic Mapping Strategy

The sine chaotic mapping model is recognized for exhibiting a higher degree of chaotic behavior compared to the logistic chaotic mapping model [36]. The mathematical formula for sine chaotic mapping used in this paper is provided in Eq. (21).

$$\begin{cases} y_{n+1} = \sin \frac{2}{y_n}, n = 0, 1, \dots, N \\ -1 < y_n < 1, y_n \neq 0 \end{cases} \quad (21)$$

As shown in Fig. 4, the sine chaotic mapping demonstrates a more uniform distribution. This improved distribution enhances the algorithm's performance, leading to faster convergence.

#### 3.3.2 Cosine Adjustment of the Formula Factor

In the FFA calculation, let  $W$  be defined by Eq. (16). As the number of iterations ( $t$ ) increases,  $W$  gradually decreases. This property allows the Fennec fox to explore a larger area initially, promoting strong global search. In later stages, as  $W$  decreases, the Fennec fox focuses on a smaller area, enhancing the local search. To further improve the global search efficiency and local search precision, a cosine adjustment is applied to the factor in Eq. (16). This adjustment is inspired by enhancements made to the dung beetle optimization algorithm [37]. The adjusted formula is presented in Eq. (22). The updated position of the Fennec fox in the first stage is given by the new formula in Eq. (23). This modified formula incorporates the cosine adjustment to balance exploration and exploitation, leading to potentially better optimization results.

$$W = 0.5 \cdot (\cos(\pi \cdot (iter/Maxiter)) + 1), \quad (22)$$

$$y_{ij}^{q1} = y_{ij} + (2 \cdot r - 1) \cdot 0.5 \cdot (\cos(\pi \cdot (iter/Maxiter)) + 1). \quad (23)$$

As shown in Fig. 5, the factor in the calculation formula for domain  $R$  before the proposed enhancement exhibits a linear variation. In contrast, the factor variation of the improved domain  $R$  is nonlinear.

#### 3.3.3 Cauchy Operator Mutation Strategy

The Cauchy distribution has a slow decline on both sides of its peak, which helps Fennec foxes reduce the constraints of local optima after mutation. To expedite the search process of Fennec foxes within the search space, DEMFFA incorporates the Cauchy operator mutation strategy. Figure 6. Illustrates the function diagram of the one-dimensional Cauchy distribution. The probability density function for the one-dimensional Cauchy distribution [38] is provided in Eq. (24).

$$f(y, \delta, \mu) = \frac{1}{\pi} \frac{\delta}{\delta^2 + (y - \mu)^2}, -\infty < y < \infty. \quad (24)$$

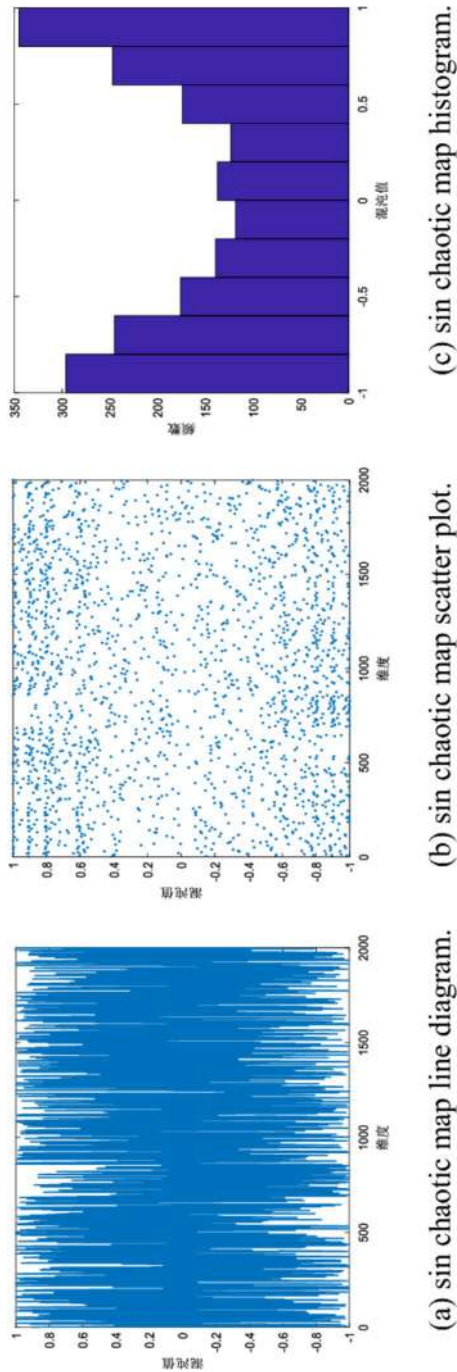
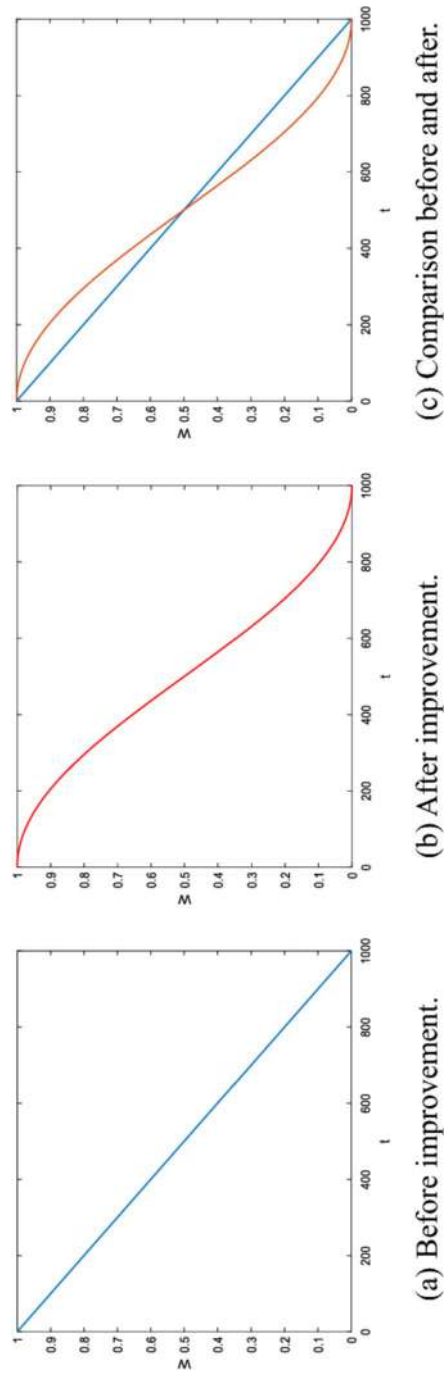
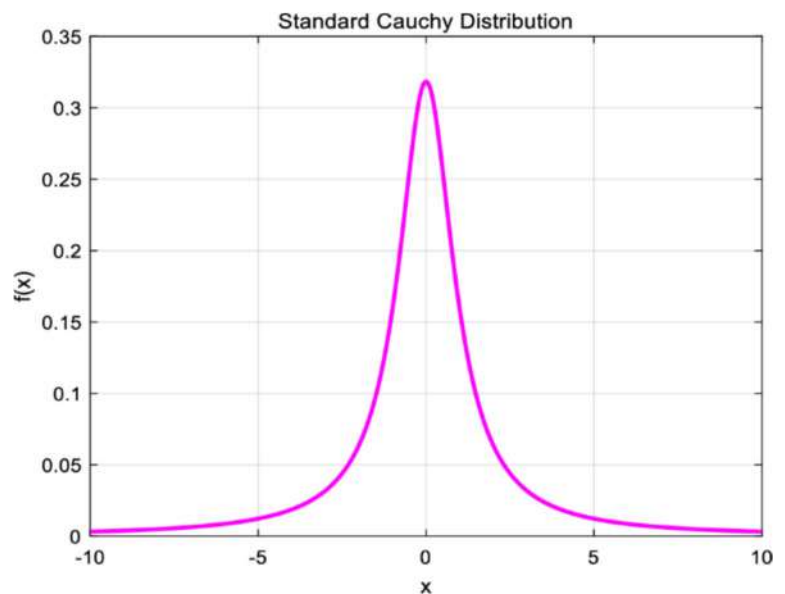


Fig. 4 Graph of sine chaotic map distribution [35]



**Fig. 5** Comparison of before and after comparison chart [35]

**Fig. 6** One-dimensional Cauchy distribution function diagram [35]



When  $\delta = 1, \mu = 0$ , the specific formula is shown in (25):

$$f(y, \delta, \mu) = \frac{1}{\pi} \frac{1}{y^2 + 1}, -\infty < y < \infty. \quad (25)$$

The formula for the standard Cauchy distribution is shown in (26):

$$Cauchy(0,1) = \tan[(\xi - 0.5)\pi], \xi \in U[0,1]. \quad (26)$$

By integrating the position update of the Fennec fox in the first stage of FFA with the variation of the Cauchy operator, the formula for generating mutant individuals is presented in Eq. (27). In DEMFFA, the updated individual in the first stage undergoes mutation by randomly adding a Cauchy operator to each dimension. This approach enhances the algorithm's ability to escape the local optima and improves its overall effectiveness in finding the global optimal solution.

$$Y_{new}(y) = Y_i + \beta \cdot Cauchy(0,1), \quad (27)$$

where  $\beta$  is the disturbance factor, which is set to 0.1 in this article.

### 3.4 Differential Evolutionary Variation Strategy

Differential evolution (DE) is a real-coded evolutionary algorithm for optimization, introduced by Storn and Price in 1995. Its core mechanism involves weighting two randomly selected vectors and adding them to a third random vector to generate a new vector [39]. DE iteratively improves candidate solutions through evolutionary principles [40]. The main operations of DE are:

#### (1) Variation operation

In the variation stage, the variation formula for new individuals is as follows (28):

$$v_i(g+1) = x_{r_1}(g) + F \cdot (x_{r_2}(g) - x_{r_3}(g)), i \neq r_1 \neq r_2 \neq r_3, \quad (28)$$

where  $F$  is the scaling factor. Figure 7a. shows the schematic diagram of the mutation operation.

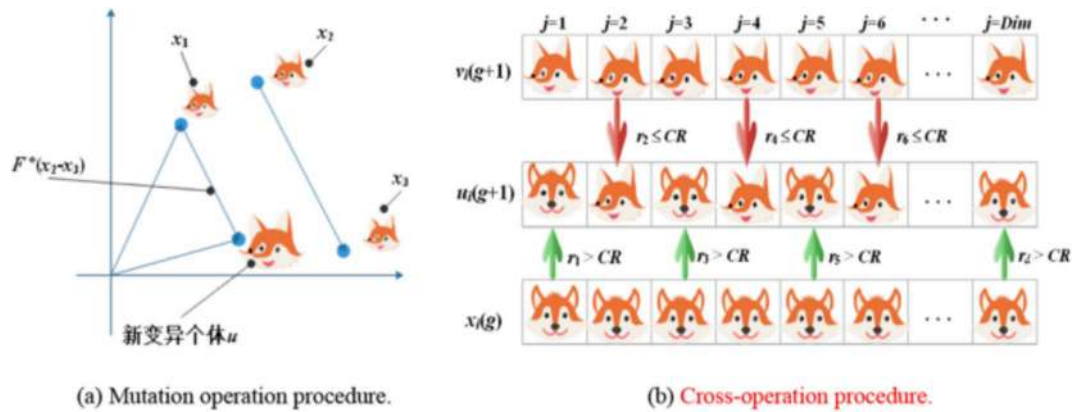


**Fig. 7** Differential evolution algorithm operation diagram [35]

Some of the previously improved DE are based on Eq. (28), and some are based on Eq. (29):

$$v_i(g+1) = x_{r1}(g) + F_1 \cdot (x_{best}(g) - x_{r1}(g)) + F_2(x_{r2}(g) - x_{r3}(g)). \quad (29)$$

In DEMFFA, the formula used for mutation operation is shown in (30):

$$v_i(g+1) = x_{r1}(g) + F \cdot ((x_{r2}(g) - x_{r3}(g)) + (x_{r4}(g) - x_{r5}(g))). \quad (30)$$

In the formula (29),  $i \neq r_1 \neq r_2 \neq r_3 \neq r_4 \neq r_5$ , the scaling factor is calculated as follows (31):

$$F = F_{max} - (iter/Maxiter) \cdot (F_{max} - F_{min}), \quad (31)$$

where  $F_{max}$  is 0.9 and  $F_{min}$  is 0.4.

## (2) Cross operation

The  $g$  generation population and its variant intermediate individual were cross operated, the formula for the cross operation is shown in (32):

$$u_{ij}(g+1) = \begin{cases} v_{ij}(g+1), & \text{rand}(0,1) \leq CR \text{ or } j = j_{rand} \\ x_{ij}(g), & \text{otherwise} \end{cases} \quad (32)$$

where CR is the crossover probability, and crossover operation uses the crossover probability CR to select  $\{x_i(g)\}$  or  $\{v_i(g+1)\}$  as the allele of  $\{u_i(g+1)\}$ ,  $j_{rand}$  is a random integer  $[1, 2, \dots, D]$ , and Fig. 7b. Shows the cross-operation diagram.

In this paper, the CR calculation formula is shown as (33):

$$CR = CR_{max} - (CR_{max} - CR_{min}) \cdot (iter/Maxiter), \quad (33)$$

where,  $CR_{max} = 1$ ,  $CR_{min} = 0$ , iter is the current iteration number, and Maxiter is the total iteration number.

## (3) Selection operation



After performing the mutation and crossover operations, differential evolution (DE) uses a greedy approach to select the next generation of individuals. This selection process evaluates both the original individuals and those generated through the crossover operation, ensuring that the fittest individuals are carried forward. The mathematical formula used in this selection operation is provided in Eq. (34).

$$x_i(g+1) = \begin{cases} u_i(g+1), & f(u_i(g+1)) \leq f(x_i(g)) \\ x_i(g) & \text{otherwise} \end{cases} \quad (34)$$

By incorporating the differential evolution mutation strategy into the second stage of the FFA, the search range of the Fennec foxes is expanded. This helps prevent the algorithm from prematurely stagnating and enhances its ability to escape local optima, thereby improving overall optimization performance. According to DEMFFA's steps, its pseudo-code is shown in Algorithm 2. In addition, Fig. 8. Shows the flowchart of DEMFFA.

### 3.5 DEMFFA Algorithm Complexity

The FFA suffers from limitations such as slow convergence, sensitivity to initial conditions, and a tendency to get trapped in suboptimal solutions. To overcome these challenges, this research introduces several enhancements. Sine chaotic mapping diversifies the initial search directions, improving exploration. Cosine adjustment dynamically refines the search path, preventing stagnation and enhancing local search. Cauchy mutation introduces greater diversity in the later stages, enabling the algorithm to escape local optima and discover superior global solutions. These enhancements collectively address the inherent weaknesses of the original FFA, resulting in improved performance and more robust solutions in complex optimization scenarios. To mitigate the deficiencies of DEMFFA and improve its performance, researchers often employ hybrid approaches that combine it with other optimization techniques. For example, combining DEMFFA with a local search algorithm can help it escape local optima and find better solutions. Additionally, adaptive parameter tuning strategies can be used to dynamically adjust parameters during the optimization process. It's important to note that the effectiveness of DEMFFA depends on the specific problem being solved and the implementation details. By carefully considering these factors and employing appropriate techniques, DEMFFA can be a valuable tool for optimizing SOFC models and other complex systems. The analysis of algorithm complexity is an approximate estimate rather than an exact calculation. The original FFA is enhanced with the following stages:

- Initialization: Sine chaotic mapping is incorporated to process the initial population, with the complexity of this stage denoted as  $O(Ini)$ .
- First stage: Cosine adjustment of the formula factor is added, and the complexity of this stage is denoted as  $O(\cos - adjustment)$ .
- Before the end of the first stage: The Cauchy operator mutation strategy is applied, with the complexity of this stage denoted as  $O(Cauchy)$ .
- Second stage: After the second stage, the differential evolution mutation strategy is incorporated, with the complexity of this stage denoted as  $O(DE)$ .

$$\begin{aligned} O(DEMFFA) &= O(definition) + O(Ini) + O(t(f)) + O(\cos - adjustment) + O(Cauchyoperator) + O(DE) \\ &= O(1 + (ND + ND) + TND + ND + TND + TND) \\ &= O(1 + 3ND + 3TND). \end{aligned}$$

Algorithm-2 [36]:

Begin DEMFFA			
		Step 1: Initialization: set the $pop$ , $T$ , $Dim$ , and initialize the population using Eq. (3.1). Set the $t$ to 1;	
		Step 2: Fitness calculation: Calculate the fitness value $f$ of each Fennec fox, and select the current best individual $Y_{best}$ based on the size of the fitness value. The corresponding optimal fitness value for this individual $f_{best}$ ;	
		Step 3: While $iter$ is less than the $Maxiter$	
		for $i = 1$ to $pop$ do	
			$R_{i,j} = \alpha \cdot ((\cos(\pi \cdot (iter/Maxiter)) + 1) \cdot 0.5) \cdot y_{i,j}$
			$Y_{new} = y_{i,j} + (2 \cdot r - 1) \cdot R(i,:)$
			if $f(Y_{new}) < f(Y_{best})$
			$Y_{best} = Y_{new}; f_{best} = f(Y_{new})$
			end if
			$u_{new} = y_{i,j} + \beta \cdot Cauchy(0,1)$
			if $f(Y_{u_{new}}) < f(Y_{best})$
			$Y_{best} = Y_{u_{new}}; f_{best} = f(Y_{u_{new}})$
			end if
		end for	
		$Y_{rand} = rand(Pop, Dim) \cdot y$	
		$I = I + rand$	
		for $i = 1$ to $pop$ do	
			Calculate the fitness value of $Y_{rand}$
			if $f(Y_{rand}) < f(Y_{best})$
			$Y_{new} = y_{i,j} + rand \cdot (y_{rand} - I \cdot y_{i,j})$
			else
			$Y_{new} = y_{i,j} + rand \cdot (y_{i,j} - y_{rand})$
			else if
			if $f(Y_{new}) < f(Y_{best})$
			$Y_{best} = Y_{new}; f_{best} = f(Y_{new})$
			end if
		end for	
		for $i = 1$ to $pop$ do	
			for $j = 1$ to $Dim$ do
			$Y_{new} = y_{r1} + F \cdot ((y_{r2} - y_{r3}) + (y_{r4} - y_{r5}))$
			if $rand < CR$
			$Y_{positions} = Y_{new}$
			else
			$Y_{positions} = Y_{best}$
			end if
		end for	
		end for	
		for $i = 1$ to $pop$ do	
			if $f(Y_{positions}) < f(Y_{best})$
			$Y_{best} = Y_{positions}; f_{best} = f(Y_{positions})$
			end if
		end for	
		end While	
		Step 4: Return: The optimal position $Y_{best}$ and fitness value $f(Y_{best})$ for Fennec Fox	
		End DEMFFA	

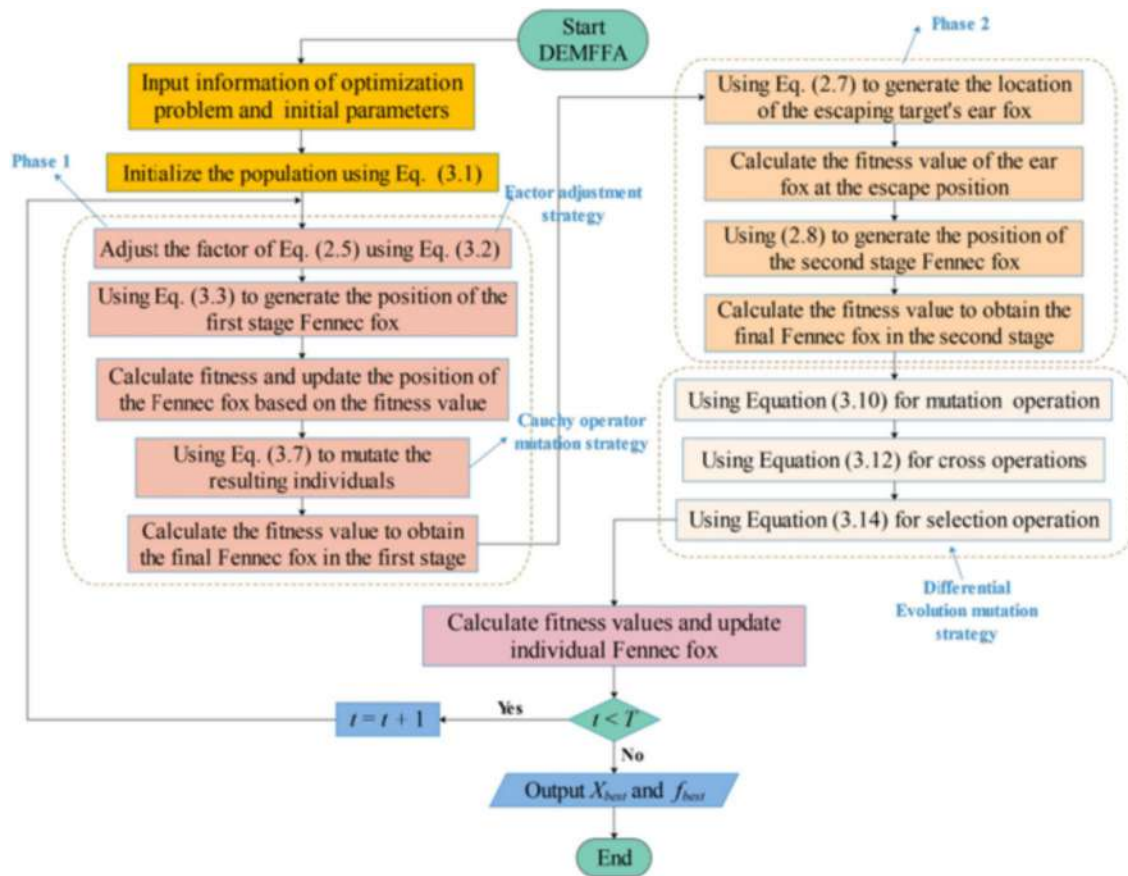


Fig. 8 DEMFFA's flowchart [35]

This research introduces DEMFFA, a novel optimization algorithm specifically designed for enhancing SOFC models. Unlike existing methods, DEMFFA incorporates advanced mechanisms like sine chaotic mapping (broad initial exploration), cosine adjustment (focused local search), and Cauchy mutation (preventing stagnation) to effectively balance exploration and exploitation. This leads to improved model accuracy and efficiency, with superior performance demonstrated in real-world scenarios. Future research will extend DEMFFA's application to other fuel cell types (proton exchange membrane fuel cell (PEMFCs), molten carbonate fuel cell (MCFCs)), integrate it with renewable energy sources in hybrid systems, and develop multi-objective optimization frameworks to address efficiency, cost, and environmental impact simultaneously.

## 4 Results and Discussion

To evaluate the performance of our new DEMFFA algorithm, we compare it to several established methods including honey badger algorithm (HBA), particle swarm optimizer (PSO), salp swarm algorithm (SSA), heap based optimizer (HBO), and Fennec fox algorithm (FFA) [41–44]. Table 1 details the specifications of the SOFC stack used for testing, and Table 2 shows the range of possible values for its control variables ( $E_0$ ,  $A$ ,  $J_{o,a}$ ,  $J_{o,c}$ ,  $b$ ,  $J_{max}$ , and  $R_{ohm}$ ). The goal of this optimization process is to find the best settings for these control variables that

**Table 1** SOFC technical data overview

Model	Data
Number of cells in stacks $n_{\text{cell}}$	96
Oxygen partial pressure	0.21
Reactants	Hydrogen and air
Stack temperature (K)	923
Hydrogen partial pressure	0.9
Power rated	5
Water partial pressure	0.1
Pressure bar	3

**Table 2** Bounds of SOFC

Parameters	Lower bound	Upper bound
$E_o$ (V)	0	1.2
$R_{\text{ohm}}$ (k-ohm- $\text{m}^2$ )	0	1
$b$ (V)	0	1
$A$ (V)	0	1
$J_{\text{max}}$ (mA/ $\text{cm}^2$ )	0	1000
$J_{o,a}$ (mA/ $\text{cm}^2$ )	0	100
$J_{o,c}$ (mA/ $\text{cm}^2$ )	0	100

minimize the difference between the predicted voltage from our model and actual voltage measurements taken at various current levels. Essentially, we are fine-tuning the model to achieve the most accurate representation of the SOFC stack's behavior.

#### 4.1 Parameter Estimation of SOFC

The author implemented all algorithms, including the proposed algorithm (DEMFFA), in MATLAB 2020a and ran them 40 times each. Our main focus was to compare DEMFFA performance in estimating SOFC parameters against established methods (HBA, PSO, SSA, HBO, FFA). Table 3 summarizes the results at standard temperature conditions (923 K), showing both the sum of squared error (SSE) and computation time. Figures 9, 10, and 11 visually represent these results, confirming that DEMFFA achieves lower SSE, lower multi-radar error axis, and faster computation times compared to other algorithms. Statistical results for the SOFC are presented in Table 4.

#### 4.2 Convergence Analysis

Tables 5 and 6 present the estimated parameters for the SOFC model at various operating temperatures and pressures, respectively. To assess the effectiveness of the proposed algorithm, the corresponding SSE (sum of squared error) and computation time are visualized in Figs. 12, 13, 14, 15. These results demonstrate that the proposed algorithm consistently achieves high accuracy (low SSE) and efficiency (fast computation time) across different operating conditions. Table 5 shows the parameter estimation at different operating temperatures of SOFC, i.e., 973 K, 1023 K, and 1073 K, and Table 6 shows the parameter estimation at different operating pressure of SOFC, i.e., 4 atm, 5 atm, and 6 atm. DEMFFA consistently achieved lower SSE values compared to other methods, demonstrating superior adaptability. The algorithm's robustness is attributed to its ability to dynamically adjust exploration and exploitation mechanisms, maintaining high accuracy even under challenging conditions.

### 4.3 Parametric-Free Statistical Analysis

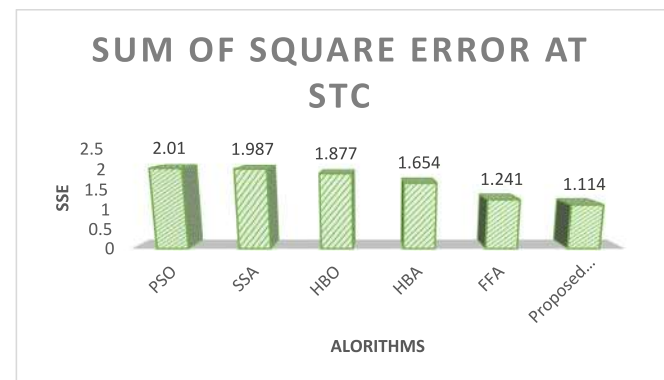
Statistical analysis confirms that the proposed DEMFFA algorithm significantly outperforms other methods for SOFC parameter estimation. This is evident in Table 7, which shows the Friedman ranking test results, where DEMFFA achieves the top rank, followed by PO, TSO, ASO, GWO, and SCA (visualized in Fig. 16) [45–47]. The Wilcoxon rank sum test, a reliable non-parametric method for independent samples, further validates these findings (results in Table 8). Overall, these tests demonstrate the superior efficiency, accuracy, precision, and robustness of the ETSO algorithm compared to existing techniques.

The results highlight that the improved parameter estimation leads to better predictive accuracy of the SOFC models. This enables more efficient system designs, reduced operational losses, and optimized fuel utilization

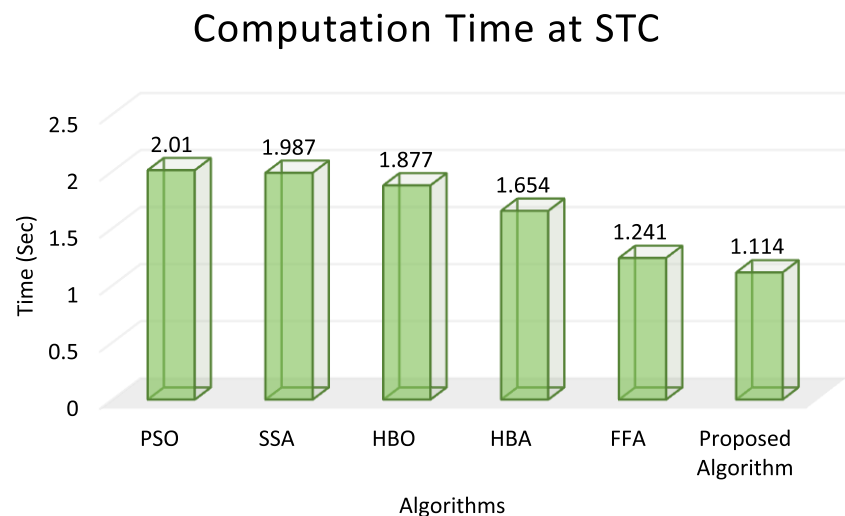
**Table 3** SOFC parameter evaluation

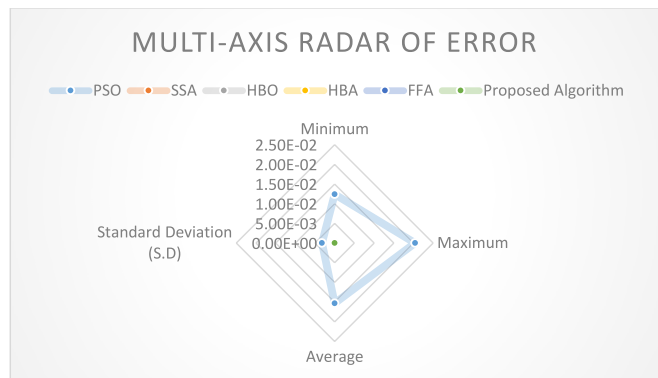
Parameters/algorithms	PSO	SSA	HBO	HBA	FFA	Proposed algorithm
$E_o$	1.1587	1.0586	1.1527	1.1569	1.1524	1.1465
$R_{ohm}$	0.0017	0.0043	0.0024	0.0031	0.0028	0.0014
$b$	0.0147	0.0253	0.0247	0.0217	0.0298	0.0175
$A$	0.0347	0.0250	0.0241	0.0297	0.0201	0.0310
$J_{max}$	147	190	287	324	310	254
$J_{o,a}$	21.1587	18.2571	22.6524	17.2107	19.5278	22.6354
$J_{o,c}$	9.5874	9.6521	9.2541	8.5621	8.3247	8.6017
SSE	1.24E-02	1.20E-04	2.01E-05	1.24E-06	1.24E-09	1.18E-11
Computation time (S)	2.651	2.304	2.011	1.207	1.199	1.001

**Fig. 9** SSE at STC



**Fig. 10** Computation time at STC



**Fig. 11** Multi-axis radar of error at STC**Table 4** Statistical results of SOFC at STC

Parameters/algorithms	PSO	SSA	HBO	HBA	FFA	Proposed algorithm
Minimum	1.24E-02	1.20E-04	2.01E-05	1.24E-06	1.24E-09	1.18E-11
Maximum	2.04E-02	2.25E-04	2.31E-05	2.01E-06	2.64E-09	1.65E-11
Average	1.53E-02	1.60E-04	2.14E-05	1.51E-06	1.70E-09	1.34E-11
Standard deviation (S.D)	3.23E-03	3.99E-05	1.14E-06	3.00E-07	5.62E-10	1.85E-12

**Table 5** Parameter estimation of SOFC at different operating temperatures

Temperature (K)	Parameters/algorithms	PSO	SSA	HBO	HBA	FFA	Proposed algorithm
973	$E_o$	1.1248	1.0652	1.1247	1.1267	1.0289	1.1572
	$R_{ohm}$	0.0054	0.0015	0.0065	0.0031	0.0037	0.0034
	b	0.0154	0.0548	0.0315	0.0217	0.0297	0.0147
	A	0.0267	0.0235	0.0387	0.0357	0.0524	0.0486
	$J_{max}$	147	204	268	197	278	301
	$J_{o,a}$	12.5478	21.1247	19.5321	15.6854	23.4218	17.6534
	$J_{o,c}$	6.87	5.49	6.87	5.47	6.37	5.24
	SSE	1.14E-02	1.26E-04	3.14E-05	1.41E-06	1.62E-09	1.36E-11
1023	Computation time (S)	2.745	2.427	2.018	1.350	1.157	1.056
	$E_o$	1.0475	1.1574	1.0657	1.0472	1.1470	1.0482
	$R_{ohm}$	0.0047	0.0021	0.0049	0.0024	0.0057	0.0017
	b	0.0421	0.0524	0.0587	0.0657	0.0354	0.0247
	A	0.0287	0.0678	0.0357	0.0258	0.0574	0.0847
	$J_{max}$	178	214	175	241	170	187
	$J_{o,a}$	14.8742	20.6847	14.5278	21.5842	34.2014	11.5841
	$J_{o,c}$	6.57	5.84	6.34	7.24	6.41	6.52
1073	SSE	1.20E-02	1.37E-04	3.05E-05	1.29E-06	1.24E-09	1.11E-11
	Computation Time (Sec)	2.634	2.247	2.017	1.207	1.127	1.112
	$E_o$	1.0621	1.0147	1.0354	1.1485	1.1357	1.1684
	$R_{ohm}$	0.0247	0.0241	0.0621	0.0157	0.0042	0.0058
	b	0.0354	0.0257	0.0287	0.0254	0.0234	0.0524
	A	0.0247	0.0254	0.0635	0.0324	0.0541	0.0342
	$J_{max}$	114	155	251	187	295	351
	$J_{o,a}$	14.5247	19.3642	15.2574	24.6587	16.3207	28.9654
	$J_{o,c}$	6.87	5.21	4.67	6.21	7.86	6.24
	SSE	1.65E-02	2.28E-04	2.41E-05	1.91E-06	2.04E-09	1.52E-11
	Computation time (S)	2.759	2.211	2.014	1.231	1.114	1.021



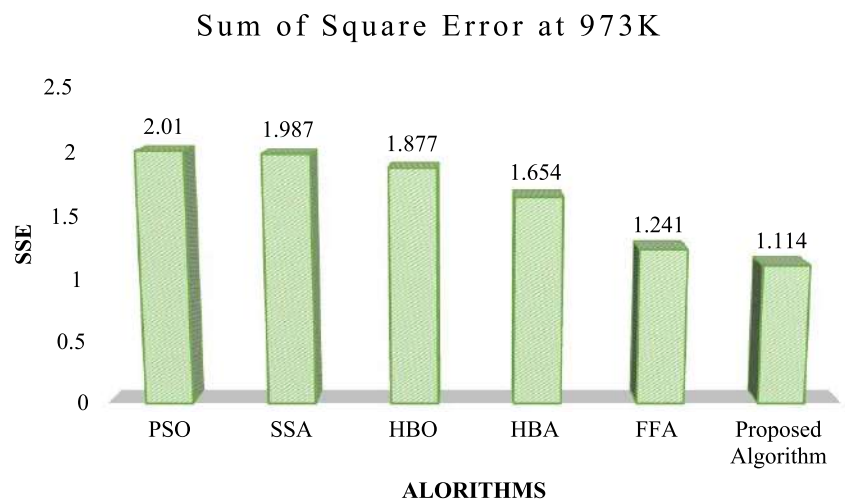
**Table 6** Parameter estimation of SOFC at different pressures

Pressure (atm)	Parameters/algorithms	PSO	SSA	HBO	HBA	FFA	Proposed algorithm
4	$E_o$	1.1249	1.1241	1.1365	1.1351	1.1257	1.1297
	$R_{ohm}$	0.0021	0.0054	0.0027	0.0030	0.0057	0.0024
	$b$	0.0478	0.0321	0.0247	0.0327	0.0429	0.0657
	$A$	0.0178	0.0167	0.0251	0.0451	0.0374	0.0248
	$J_{max}$	187	217	197	254	321	387
	$J_{o,a}$	12.2486	14.3248	17.0524	15.6524	27.6572	28.3524
	$J_{o,c}$	6.35	6.47	3.24	5.27	5.34	6.87
	SSE	1.14E-02	2.14E-04	2.35E-05	1.26E-06	1.75E-09	1.30E-11
5	Computation time (s)	2.741	2.314	2.151	1.274	1.148	1.112
	$E_o$	1.1278	1.1357	1.0547	1.1398	1.0237	1.1523
	$R_{ohm}$	0.0034	0.0027	0.0032	0.0017	0.0023	0.0020
	$b$	0.0172	0.0234	0.0320	0.0251	0.0987	0.0142
	$A$	0.0421	0.0247	0.0365	0.0324	0.0257	0.0214
	$J_{max}$	187	150	190	247	214	267
	$J_{o,a}$	14.6354	21.8541	10.3241	12.2571	19.3520	18.6527
	$J_{o,c}$	6.38	5.27	2.84	5.67	4.27	4.30
6	SSE	1.30E-02	1.07E-04	2.42E-05	1.31E-06	1.11E-09	1.14E-11
	Computation time (s)	2.421	2.315	2.014	1.200	1.121	1.110
	$E_o$	1.1325	1.1147	1.0410	1.1452	1.1207	1.1209
	$R_{ohm}$	0.0014	0.0052	0.0024	0.0031	0.0017	0.0029
	$b$	0.0175	0.0231	0.0421	0.0357	0.0318	0.0241
	$A$	0.0145	0.0243	0.0189	0.0501	0.0284	0.0349
	$J_{max}$	178	152	204	256	220	208
	$J_{o,a}$	14.3257	21.5241	08.2372	22.3527	17.6501	27.6824
	$J_{o,c}$	6.35	7.42	6.28	5.01	3.27	3.65
	SSE	1.41E-02	1.37E-04	2.07E-05	1.47E-06	1.58E-09	1.31E-11
	Computation time (s)	2.754	2.214	2.119	1.354	1.021	1.010

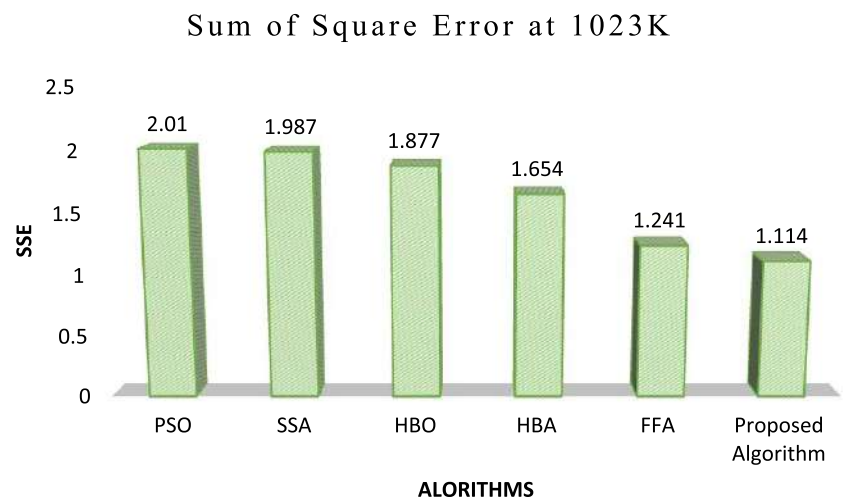
in real-world energy systems, such as distributed power generation and hydrogen production facilities. These advancements contribute directly to cost savings and increased system reliability in practical applications.

## 5 Discussion

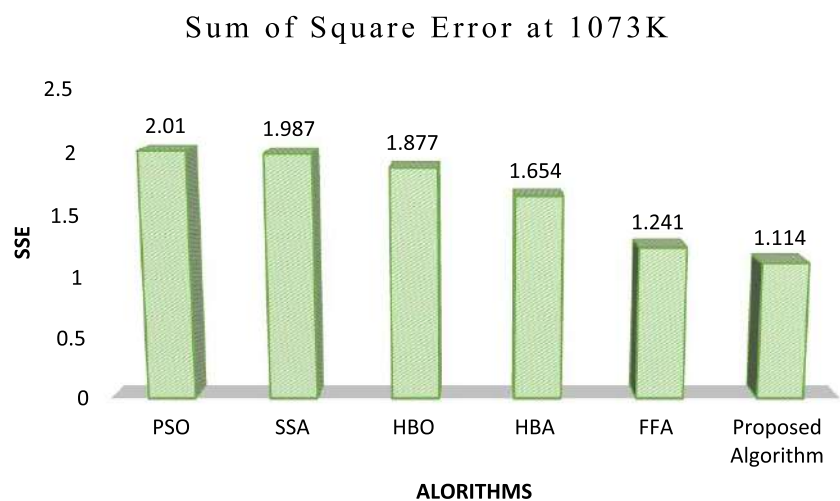
This research proposes a novel optimization approach, the DEMFFA, specifically designed for enhancing SOFC models. Unlike existing methods like multi-objective equilibrium optimizer slime mold algorithm (MOEOSMA), adaptive operator selection with dueling deep Q-network (AOSDDQN), adaptive differential evolution (ADE-DYTS), and hyper-heuristic algorithm via proximal policy optimization (HHEA-PPO) [48–51], which primarily address multi-objective engineering, UAV path planning, and truss optimization, DEMFFA is uniquely tailored to the complexities of SOFC systems. DEMFFA incorporates advanced mechanisms such as sine chaotic mapping, cosine adjustment, and Cauchy mutation to effectively balance exploration and exploitation during the optimization process. This results in improved model accuracy and efficiency, leading to more reliable predictions and better adaptability to varying operating conditions (temperature, pressure). The research demonstrates the superior performance of DEMFFA in real-world scenarios, surpassing existing approaches in addressing the specific challenges of SOFC modeling and optimization within energy systems, such as also shown in Table 9.

**Fig. 12** SSE at different operating temperature

(a)

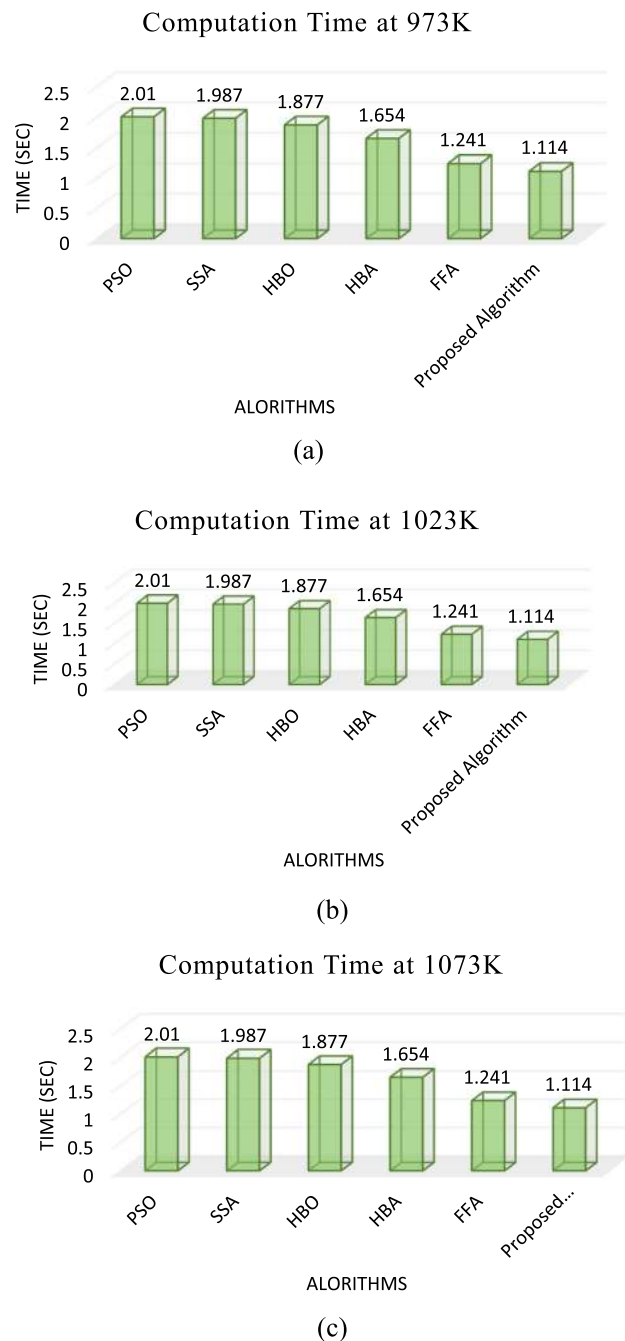


(b)



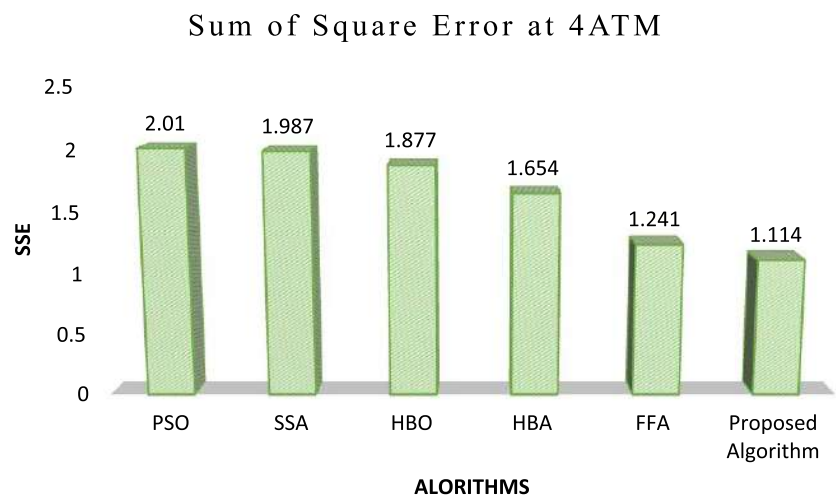
(c)

**Fig. 13** Computation time at different operating temperatures

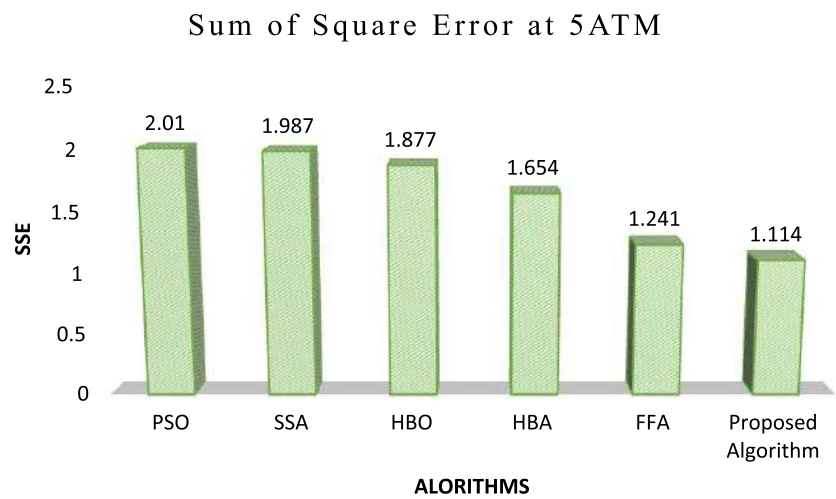


## 6 Conclusions

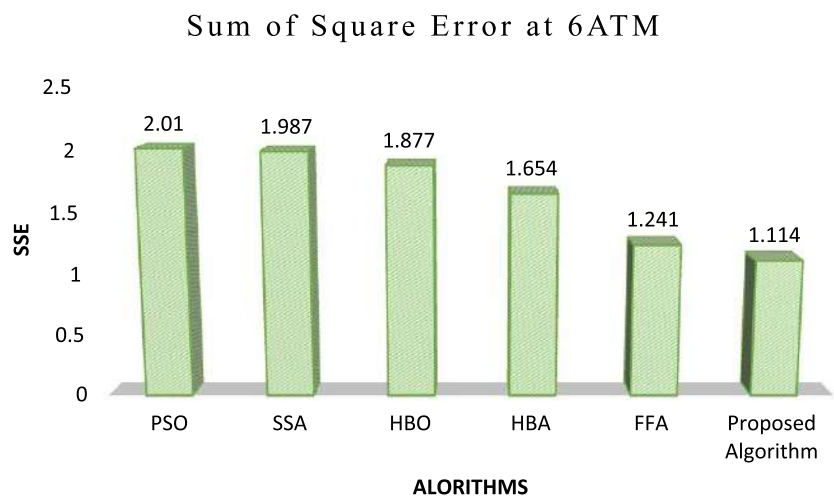
The current focus is on developing more efficient energy sources and power generation methods, with solid oxide fuel cells (SOFCs) emerging as a promising option. SOFCs operate at high temperatures, which makes them more cost-effective to produce compared to other types of fuel cells. However, they require specific operating conditions and carefully designed systems. A notable advantage of SOFCs is their ability to utilize waste heat, which can be employed in reformers to produce hydrogen when direct access to it is limited or too costly. This versatility

**Fig. 14** SSE at different pressures

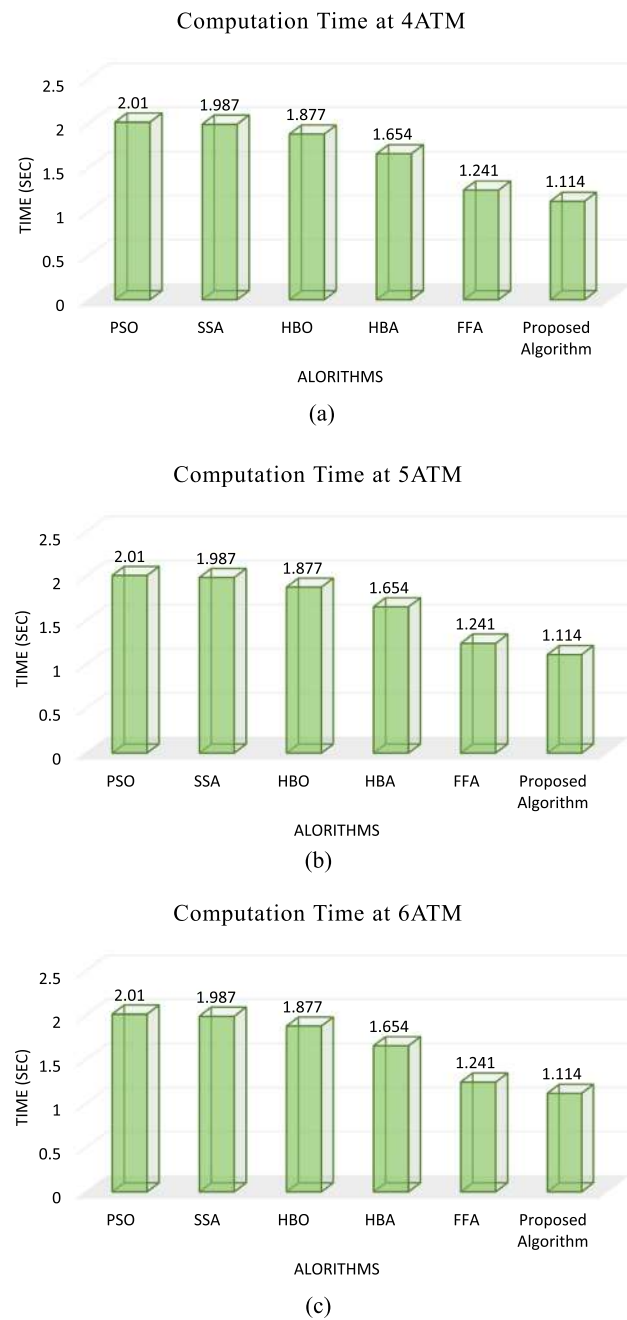
(a)



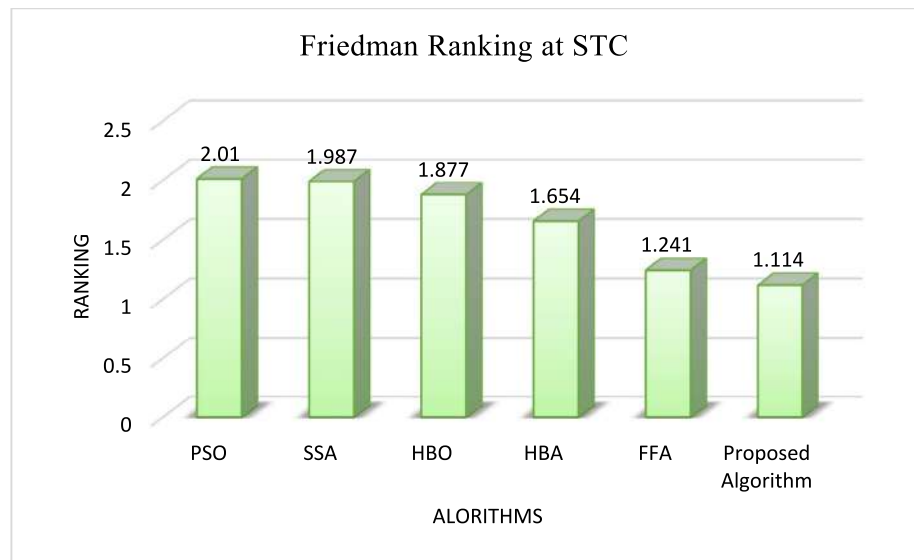
(b)



(c)

**Fig. 15** Computation time at different pressures

**Table 7** Friedman ranking test

Algorithm	Friedman ranking	Ranking
Proposed algorithm	1.114	1
FFA	1.241	2
HBO	1.654	3
HBA	1.877	4
SSA	1.987	5
PSO	2.010	6

**Fig. 16** Friedman ranking at STC**Table 8** Wilcoxon rank sum test

Algorithm	FFA	HBO	HBA	SSA	PSO
Proposed algorithm	2.0514E-11	3.0247E-11	3.0527E-11	3.0354E-11	2.5479E-11

distinguishes SOFCs from other fuel cells. Mathematical modeling plays a critical role in optimizing SOFCs before they are constructed, helping to avoid expensive errors. This study introduces a novel and effective approach for identifying SOFC parameters, using voltage and power data to ensure accuracy. The approach employs an optimization technique based on a modified metaheuristic algorithm known as the proposed algorithm (DEMFFA) to determine the optimal parameters for the model. By minimizing the sum of squared errors (SSE) between the model's predicted voltage and actual experimental data, the model's accuracy is enhanced. The proposed model's effectiveness is then validated under various pressure and temperature conditions in a real-world scenario, with results compared to other techniques. The final outcomes show a strong correlation between real-world data and the model's predictions, confirming the validity of the proposed modeling approach.

## 7 Future Work

Future research avenues include expanding the DEMFFA algorithm's applicability to diverse fuel cell technologies, such as PEMFCs and DMFCs, to evaluate its robustness and generalizability. Incorporating real-time data and dynamic environmental factors into the parameter estimation process would enhance the algorithm's adaptability to real-world conditions. Hybridizing DEMFFA with machine learning techniques could enable predictive degradation modeling and optimized performance over the fuel cell's lifespan. Finally, integrating DEMFFA into embedded systems would facilitate real-time control and monitoring of SOFCs, paving the way for efficient, automated fuel cell management in practical applications.



**Table 9** Comparison table with respect to other previous studies

S. No	Feature	Previous studies			Proposed work on DEMFFA for SOFC optimization
		MOEOSMA [48]	DDQN for MO optimization [49]	DE-DYTS for UAV path planning [50]	HHEA-PPO for Truss problems [51]
1	Objective	Multi-objective optimization problems using slime mold algorithm	Adaptive operator selection in multi-objective optimization with DDQN for efficiency	Path planning for multiple UAVs using adaptive differential evolution	Multi-objective optimization for truss design using hyper-heuristic and PPO
2	Methodology	MOESMA with dynamic coefficients, elite archiving, and equilibrium pool strategy	Dueling deep Q-network (DDQN) for adaptive operator selection with adaptive weights	DE-DYTS using dynamic Thompson sampling and differential evolution operators	Hyper-heuristic approach using PPO for operator selection in multi-objective truss problems
3	Contribution	Improved multi-objective slime mold algorithm (MOEOSMA) for better convergence, diversity, and uniformity	Proposal of a DDQN-based adaptive operator selection to improve multi-objective optimization	Introduction of DE-DYTS combining differential evolution and Thompson sampling for UAV path planning	HHEA-PPO integrates PPO with predefined heuristics for solving truss optimization problems
4	Performance	Convergence, diversity, uniformity, and extensiveness, showing superior performance over other algorithms	Performance improvement in terms of optimization efficiency and adaptability	Efficiency and effectiveness in UAV path planning with a focus on coordination and collision avoidance	Higher search efficiency and stability for large-scale engineering design problems
5	Evaluation criteria	Evaluated on CEC2020 functions, multi-objective engineering problems, and truss optimization	Tested on three benchmark suites to evaluate the performance improvement	Evaluated on path planning scenarios for UAVs with statistical analysis using Wilcoxon test	Applied to eight truss optimization problems and compared with state-of-the-art algorithms
6	Application	Engineering optimization (multi-objective constraint problems, large-scale truss structures)	Multi-objective evolutionary optimization in complex environments	UAV collaborative path planning with focus on coordination and avoiding collisions	Truss design optimization in multi-objective settings
7	Novelty as per authors' studies	MOEOSMA finds more Pareto optimal solutions and maintains a good distribution in decision and objective spaces	AdaW-DDQN significantly improves the performance of multi-objective optimization algorithms	DE-DYTS outperforms advanced DE variants, especially in scenarios with many UAVs	HHEA-PPO shows higher stability and search efficiency in large-scale problems
					Validated through a real-world case study, comparing model accuracy under varying conditions
					Solid Oxide Fuel Cell (SOFC) model optimization for energy systems
					DEMFFA provides a more accurate and efficient model for SOFCs, outperforming existing methods

**Acknowledgements** The authors acknowledge Princess Nourah bint Abdulrahman University Researchers Supporting Project number (PNURSP2025R120), Princess Nourah bint Abdulrahman University, Riyadh, Saudi Arabia.

**Author Contributions** M.K. Singla: Conceptualization, Methodology, Writing-original draft. J. Gupta: Formal analysis, Validation, Writing-review & editing. R. Kumar: Methodology, Formal analysis. P Jangir: Investigation, Data curation, Writing-review & editing. El-Sayed M. El-Kenawy; M. Louzazni: Visualization, Supervision. Amal H. Alharbi; Nimay Chandra Giri, and Ahmed Jamal Abdullah Al-Gburi: Conceptualization, Resources.

**Funding** There has been no external funding support for this study.

**Data Availability** No datasets were generated or analysed during the current study.

## Declarations

**Conflict of Interest** The authors declare no conflicts of interest.

**Ethical Approval** No ethical approval is needed.

**Open Access** This article is licensed under a Creative Commons Attribution-NonCommercial-NoDerivatives 4.0 International License, which permits any non-commercial use, sharing, distribution and reproduction in any medium or format, as long as you give appropriate credit to the original author(s) and the source, provide a link to the Creative Commons licence, and indicate if you modified the licensed material. You do not have permission under this licence to share adapted material derived from this article or parts of it. The images or other third party material in this article are included in the article's Creative Commons licence, unless indicated otherwise in a credit line to the material. If material is not included in the article's Creative Commons licence and your intended use is not permitted by statutory regulation or exceeds the permitted use, you will need to obtain permission directly from the copyright holder. To view a copy of this licence, visit <http://creativecommons.org/licenses/by-nc-nd/4.0/>.

## References

1. Aghajani, G., Ghadimi, N.: Multi-objective energy management in a micro-grid. *Energy Rep.* **4**, 218–225 (2018)
2. Akbary, P., Ghiasi, M., Pourkheranjani, M.R.R., Alipour, H., Ghadimi, N.: Extracting appropriate nodal marginal prices for all types of committed reserve. *Comput. Econ.* **53**, 1–26 (2019)
3. Cai, W., Mohammaditab, R., Fathi, G., Wakil, K., Ebadi, A.G., Ghadimi, N.: Optimal bidding and offering strategies of compressed air energy storage: a hybrid robust-stochastic approach. *Renewable Energy* **143**, 1–8 (2019)
4. Fan, X., Sun, H., Yuan, Z., Li, Z., Shi, R., Ghadimi, N.: High voltage gain DC/DC converter using coupled inductor and VM techniques. *IEEE Access* **8**, 131975–131987 (2020)
5. Firouz, M.H., Ghadimi, N.: Concordant controllers based on FACTS and FPSS for solving wide-area in multi-machine power system. *J. Intell. Fuzzy Syst.* **30**(2), 845–859 (2016)
6. Gao, W., Darvishan, A., Toghiani, M., Mohammadi, M., Abedinia, O., Ghadimi, N.: Different states of multi-block based forecast engine for price and load prediction. *Int. J. Electr. Power Energy Syst.* **104**, 423–435 (2019)
7. Bahmanyar, D., Razmjooy, N., Mirjalili, S.: Multi-objective scheduling of IoT-enabled smart homes for energy management based on Arithmetic Optimization Algorithm: A Node-RED and NodeMCU module-based technique. *Knowl.-Based Syst.* **247**, 108762 (2022)
8. Ebrahimi, H., Barmayoon, S., Mohammadi, M., Ghadimi, N.: The price prediction for the energy market based on a new method. *Econ. Res.-Ekon. Istraž.* **31**(1), 313–337 (2018)
9. Ghadimi, N., Akbarimajd, A., Shayeghi, H., Abedinia, O.: Two stage forecast engine with feature selection technique and improved meta-heuristic algorithm for electricity load forecasting. *Energy* **161**, 130–142 (2018)
10. Gheydi, M., Nouri, A., Ghadimi, N.: Planning in microgrids with conservation of voltage reduction. *IEEE Syst. J.* **12**(3), 2782–2790 (2016)
11. Yuan, Z., Wang, W., Wang, H., Ghadimi, N.: Probabilistic decomposition-based security constrained transmission expansion planning incorporating distributed series reactor. *IET Gener. Transm. Distrib.* **14**(17), 3478–3487 (2020)
12. Gong, W., Razmjooy, N.: A new optimisation algorithm based on OCM and PCM solution through energy reserve. *Int. J. Ambient Energy* **43**(1), 2299–2312 (2022)
13. Zhi, Y., Weiqing, W., Haiyun, W., Razmjooy, N.: New approaches for regulation of solid oxide fuel cell using dynamic condition approximation and STATCOM. *Int. Trans. Electr. Energy Syst.* **31**(2), e12756 (2021)
14. Zhang, G., Xiao, C., Razmjooy, N.: Optimal operational strategy of hybrid PV/wind renewable energy system using homer: a case study. *Int. J. Ambient Energy* **43**(1), 3953–3966 (2022)

15. Gollou, A.R., Ghadimi, N.: A new feature selection and hybrid forecast engine for day-ahead price forecasting of electricity markets. *J. Intell. Fuzzy Syst.* **32**(6), 4031–4045 (2017)
16. Hamian, M., Darvishan, A., Hosseinzadeh, M., Lariche, M.J., Ghadimi, N., Nouri, A.: A framework to expedite joint energy-reserve payment cost minimization using a custom-designed method based on mixed integer genetic algorithm. *Eng. Appl. Artif. Intell.* **72**, 203–212 (2018)
17. Reddy, B.K., Giri, N.C., Yemula, P.K., Agyekum, E.B., Arya, Y.: Optimal operation of cogeneration power plant integrated with solar photovoltaics using DLS-WMA and ANN. *Int. J. Energy Res.* **2024**(1), 5562804 (2024)
18. Leng, H., Li, X., Zhu, J., Tang, H., Zhang, Z., Ghadimi, N.: A new wind power prediction method based on ridgelet transforms, hybrid feature selection and closed-loop forecasting. *Adv. Eng. Inform.* **36**, 20–30 (2018)
19. Bagal, H.A., Soltanabad, Y.N., Dadjuo, M., Wakil, K., Zare, M., Mohammed, A.S.: SOFC model parameter identification by means of Modified African Vulture Optimization algorithm. *Energy Rep.* **7**, 7251–7260 (2021)
20. Yu, D., Wang, Y., Liu, H., Jermisittiparsert, K., Razmjoo, N.: System identification of PEM fuel cells using an improved Elman neural network and a new hybrid optimization algorithm. *Energy Rep.* **5**, 1365–1374 (2019)
21. Cao, Y., Li, Y., Zhang, G., Jermisittiparsert, K., Razmjoo, N.: Experimental modeling of PEM fuel cells using a new improved seagull optimization algorithm. *Energy Rep.* **5**, 1616–1625 (2019)
22. Zhang, G., Xiao, C., Razmjoo, N.: Optimal parameter extraction of PEM fuel cells by meta-heuristics. *Int. J. Ambient Energy* **43**(1), 2510–2519 (2022)
23. El-Hay, E.A., El-Hameed, M.A., El-Fergany, A.A.: Steady-state and dynamic models of solid oxide fuel cells based on Satin Bowerbird Optimizer. *Int. J. Hydrogen Energy* **43**(31), 14751–14761 (2018)
24. Yang, B., Guo, Z., Yang, Y., Chen, Y., Zhang, R., Su, K., Zhang, X.: Extreme learning machine based meta-heuristic algorithms for parameter extraction of solid oxide fuel cells. *Appl. Energy* **303**, 117630 (2021)
25. Alhumade, H., Fathy, A., Al-Zahrani, A., Rawa, M.J., Rezk, H.: Optimal parameter estimation methodology of solid oxide fuel cell using modern optimization. *Mathematics* **9**(9), 1066 (2021)
26. Karamnejadi Azar, K., Kakouee, A., Mollajafari, M., Majdi, A., Ghadimi, N., Ghadamyari, M.: Developed design of battle royale optimizer for the optimum identification of solid oxide fuel cell. *Sustainability* **14**(16), 9882 (2022)
27. Bai, Q., Li, H.: The application of hybrid cuckoo search-grey wolf optimization algorithm in optimal parameters identification of solid oxide fuel cell. *Int. J. Hydrogen Energy* **47**(9), 6200–6216 (2022)
28. Yang, B., Wang, J., Zhang, M., Shu, H., Yu, T., Zhang, X., Sun, L.: A state-of-the-art survey of solid oxide fuel cell parameter identification: modelling, methodology, and perspectives. *Energy Convers. Manage.* **213**, 112856 (2020)
29. Xiong, G., Zhang, J., Shi, D., Zhu, L., Yuan, X.: Optimal identification of solid oxide fuel cell parameters using a competitive hybrid differential evolution and Jaya algorithm. *Int. J. Hydrogen Energy* **46**(9), 6720–6733 (2021)
30. Li, Y., Wu, Q., Zhu, H.: Hierarchical load tracking control of a grid-connected solid oxide fuel cell for maximum electrical efficiency operation. *Energies* **8**(3), 1896–1916 (2015)
31. Chuahy, F.D., Kokjohn, S.L.: Solid oxide fuel cell and advanced combustion engine combined cycle: a pathway to 70% electrical efficiency. *Appl. Energy* **235**, 391–408 (2019)
32. Ni, M., Leung, M.K., Leung, D.Y.: Parametric study of solid oxide fuel cell performance. *Energy Convers. Manage.* **48**(5), 1525–1535 (2007)
33. Lan, T., Strunz, K.: Multiphysics transients modeling of solid oxide fuel cells: methodology of circuit equivalents and use in EMTP-type power system simulation. *IEEE Trans. Energy Convers.* **32**(4), 1309–1321 (2017)
34. Trojovská, E., Dehghani, M., Trojovský, P.: Fennec fox optimization: a new nature-inspired optimization algorithm. *IEEE Access* **10**, 84417–84443 (2022)
35. Hu, G., Song, K., Li, X., Wang, Y.: DEMFFA: a multi-strategy modified Fennec Fox algorithm with mixed improved differential evolutionary variation strategies. *J. Big Data* **11**(1), 69 (2024)
36. Jia, J., Yuan, S., Shi, Y., Wen, J., Pang, X., Zeng, J.: Improved sparrow search algorithm optimization deep extreme learning machine for lithium-ion battery state-of-health prediction. *Iscience* **25**(4), 103988 (2022)
37. Zhu, F., Li, G., Tang, H., Li, Y., Lv, X., Wang, X.: Dung beetle optimization algorithm based on quantum computing and multi-strategy fusion for solving engineering problems. *Expert Syst. Appl.* **236**, 121219 (2024)
38. Miao, F., Yao, L., Zhao, X.: Symbiotic organisms search algorithm using random walk and adaptive Cauchy mutation on the feature selection of sleep staging. *Expert Syst. Appl.* **176**, 114887 (2021)
39. Liu, L., Wang, J., Li, J., Wei, L.: Monthly wind distribution prediction based on nonparametric estimation and modified differential evolution optimization algorithm. *Renew. Energy* **217**, 119099 (2023)
40. Khaleel, M.I.: Efficient job scheduling paradigm based on hybrid sparrow search algorithm and differential evolution optimization for heterogeneous cloud computing platforms. *Internet of Things* **22**, 100697 (2023)
41. Hashim, F.A., Houssein, E.H., Hussain, K., Mabrouk, M.S., Al-Atabany, W.: Honey Badger Algorithm: new metaheuristic algorithm for solving optimization problems. *Math. Comput. Simul.* **192**, 84–110 (2022)
42. Kennedy, J., & Eberhart, R.: Particle swarm optimization. In *Proceedings of ICNN'95-international conference on neural networks* (Vol. 4, pp. 1942–1948). IEEE. (1995)
43. Laith, A., Mohammad, S., Mohammad, A., Hamzeh, A.: Salp swarm algorithm: a comprehensive survey. *Neural Comput. Appl.* **32**(15), 11195–11215 (2020)

44. Ginidi, A.R., Shaheen, A.M., El-Sehiemy, R.A., Hasanien, H.M., Al-Durra, A.: Estimation of electrical parameters of photovoltaic panels using heap-based algorithm. *IET Renew. Power Gener.* **16**(11), 2292–2312 (2022)
45. Gupta, J., Nijhawan, P., Ganguli, S.: Optimal sizing of different configuration of photovoltaic, fuel cell, and biomass-based hybrid energy system. *Environ. Sci. Pollut. Res.* **29**(12), 17425–17440 (2022)
46. Singla, M.K., Nijhawan, P., Oberoi, A.S.: A novel hybrid particle swarm optimization rat search algorithm for parameter estimation of solar PV and fuel cell model. *COMPEL- Int. J. Comput. Math. Electr. Electr. Eng.* **41**(5), 1505–1527 (2022)
47. Singh, B., Nijhawan, P., Singla, M.K., Gupta, J., Singh, P.: Hybrid algorithm for parameter estimation of fuel cell. *Int. J. Energy Res.* **46**(8), 10644–10655 (2022)
48. Luo, Q., Yin, S., Zhou, G., Meng, W., Zhao, Y., Zhou, Y.: Multi-objective equilibrium optimizer slime mould algorithm and its application in solving engineering problems. *Struct. Multidiscip. Optim.* **66**(5), 114 (2023)
49. Yin, S., Xiang, Z.: Adaptive operator selection with dueling deep Q-network for evolutionary multi-objective optimization. *Neurocomputing* **581**, 127491 (2024)
50. Yin, S., Wang, R., Xiang, Y., & Xiang, Z.: Adaptive differential evolution for collaborative path planning of multiple unmanned aerial vehicles. In 2024 36th Chinese Control and Decision Conference (CCDC) (pp. 1521–1526). IEEE (2024)
51. Yin, S., Xiang, Z.: A hyper-heuristic algorithm via proximal policy optimization for multi-objective truss problems. *Expert Syst. Appl.* **256**, 124929 (2024)

**Publisher's Note** Springer Nature remains neutral with regard to jurisdictional claims in published maps and institutional affiliations.

## Authors and Affiliations

**Manish Kumar Singla<sup>2,3</sup> · Jyoti Gupta<sup>4</sup> · Ramesh Kumar<sup>1,5</sup> · Pradeep Jangir<sup>6,7,8</sup> · Mohamed Louzazni<sup>9</sup> · Nimay Chandra Giri<sup>10</sup> · Ahmed Jamal Abdullah Al-Gburi<sup>11,14</sup> · E. I.-Sayed M. El-Kenawy<sup>12</sup> · Amal H. Alharbi<sup>13</sup>**

✉ Manish Kumar Singla  
msingla0509@gmail.com

Jyoti Gupta  
jg118207@gmail.com

Ramesh Kumar  
rameshkumarmeena@gmail.com

Pradeep Jangir  
pkjmttech@gmail.com

Mohamed Louzazni  
louzazni.m@ucd.ac.ma

Nimay Chandra Giri  
girinimay1@gmail.com

Ahmed Jamal Abdullah Al-Gburi  
ahmedjamal@ieee.org

E. I.-Sayed M. El-Kenawy  
skenawy@ieee.org

Amal H. Alharbi  
ahalharbi@pnu.edu.sa

<sup>1</sup> Department of Interdisciplinary Courses in Engineering, Chitkara University Institute of Engineering and Technology, Chitkara University, Rajpura, Punjab, India

- <sup>2</sup> Department of Biosciences, Saveetha School of Engineering, Saveetha Institute of Medical and Technical Sciences, Chennai, Tamil Nadu 602105, India
- <sup>3</sup> Applied Science Research Center, Applied Science Private University, Amman 11931, Jordan
- <sup>4</sup> School of Engineering and Technology, K. R. Mangalam University, Gurgaon, Haryana 122003, India
- <sup>5</sup> Jadara University Research Center, Jadara University, Irbid, Jordan
- <sup>6</sup> University Centre for Research and Development, Chandigarh University, Gharuan, Mohali 140413, India
- <sup>7</sup> Department of CSE, Graphic Era Hill University. Graphic Era Deemed to be University, Dehradun, Uttarakhand 248002, India
- <sup>8</sup> Innovation Center for Artificial Intelligence Applications, Yuan Ze University, Taoyuan City, Taiwan
- <sup>9</sup> Science Engineer Laboratory for Energy, National School of Applied Sciences, Chouaib Doukkali University of El Jadida, El Jadida, Morocco
- <sup>10</sup> Department of Electronics and Communication Engineering, Centurion University of Technology and Management, Jatni, Odisha 752050, India
- <sup>11</sup> Center for Telecommunication Research and Innovation (CeTRI), Fakulti Teknologi Dan Kejuruteraan Elektronik Dan Komputer, Jalan Hang Tuah Jaya, 76100 Durian Tunggal, Melaka, Malaysia
- <sup>12</sup> School of ICT, Faculty of Engineering, Design and Information and Communication Technology (EDICT), Bahrain Polytechnic, PO Box 33349, Isa Town, Bahrain
- <sup>13</sup> Department of Computer Sciences, College of Computer and Information Sciences, Princess Nourah Bint Abdulrahman University, P.O Box 84428, 11671 Riyadh, Saudi Arabia
- <sup>14</sup> Universiti Teknikal Malaysia Melaka, Malacca, Malaysia